Modeling of Solar Cosmic Ray Events Based on Recent Observations

M. B. Baker,* R. E. Santina,* and A. J. Masley†
McDonnell Douglas Astronautics Company, Santa Monica, Calif.

In order to assess the magnitude of a solar cosmic ray event after the first particles have been detected, solar cosmic ray events models have been developed which relate a spectral parameter to a dose parameter. Spectrometer data obtained early in an event would be used to make projections of the total expected event dose and other dose parameters. Two models were considered. The first model, Epeak, relates the energy of the particles reaching maximum intensity to the percent dose remaining. It was found that the plots of energy (of protons reaching maximum intensity) vs percent dose accumulated correlated well for several of the events. The second model is based on theoretical treatments of solar cosmic ray propagation assuming isotropic diffusion. With this model the time-integrated intensity is calculated from data early in the event. The dose rate and total dose are then calculated. For most of the events analyzed, this technique gives reasonable dose projections quite early in the event.

Introduction

SOLAR cosmic rays (SCR) are energetic charged particles, mostly protons, with varying numbers of alpha particles and small numbers of heavier nuclei. The particles are most probably accelerated during solar flares in local magnetic fields near sunspots. They then propagate through interplanetary space.

High-energy solar cosmic rays (>500 Mev) were discovered in 1942. Low-energy solar cosmic rays (1 to 500 Mev) were discovered in 1957–1958 during the International Geophysical Year. It is this low-energy group which presents the potential hazard to manned space flight. Since their discovery, more than one hundred solar cosmic ray events have been observed.

Solar activity follows an 11-yr cycle. Figure 1 shows the proton intensity (>30 Mev) for a number of the major solar cosmic ray events that have occurred during the past solar cycle (cycle 19) and thus far during cycle 20. The numbers adjacent to each solar cosmic ray event denote the integrated free space dose behind 1 g cm^{-2} aluminum. The background curves show the smoothed sunspot numbers on cycle 19 (solid line) and cycle 20 (dashed line). The peak intensities for solar cosmic ray events range from less than 1 proton cm^{-2} sec^{-1} to about 10^5 protons cm^{-2} sec^{-1}. Integrated doses range from less than one rad (100 ergs of energy deposited per gram of absorber) to 4800 rad through 1 g cm^{-2} aluminum (0.37 cm Al).

The 12 November 1960 solar cosmic ray event had a "free space" dose of 4800 rad through 1 gcm^{-2} Al. This dose was calculated using the analysis of Masley and Goedeke,[1] with the energy spectrum extended to lower energy. If analysis of this event is transferred from free space to a low-altitude polar orbit, allowing for the shielding of the solid earth and the geomagnetic field, the dose behind 1 g cm^{-2} Al shielding would be 500 to 1200 rad. Although these large doses are somewhat controversial,[2,3] there is little doubt that the dose inside a typical manned vehicle could easily be a few hundred rads. It is apparent that this hazard is worth considering in any operational plan for manned space flight in polar orbit or to the moon.

In this study, the analysis and modeling effort was an attempt to relate a spectral parameter to a dose parameter. That is, particle data obtained early in the solar cosmic ray event would be used to project the total dose and other dose parameters. Two models were considered. The first, Epeak, relates the energy of the particles reaching maximum intensity and the percentage of dose received. The second model was based on theoretical treatments of solar cosmic ray propagation assuming isotropic diffusion.

Event Selection

The solar cosmic ray events that would be of use in developing models for this study are those for which sufficient detailed energy spectra are available early in the event. Those events for which such data are available are listed in

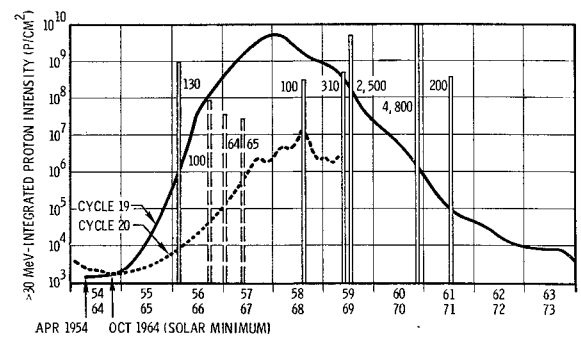

Fig. 1 Solar cosmic ray events and sunspot numbers. The solar cosmic ray events that occurred during solar cycle 19 (1954–1964) are shown as the solid vertical bars. The corresponding proton intensities (for energies >30 Mev) are shown on the vertical scale, and the dose behind 1 g cm^{-2} of Al shielding is displayed next to each event. The solid curve is the smoothed sunspot number for cycle 19. The dashed bars and dashed line are the corresponding solar cosmic ray events and sunspot numbers for cycle 20 (1964–1975).

Presented as Paper 69-14 at the AIAA 7th Aerospace Sciences Meeting, New York, January 20–22, 1969; submitted February 6, 1969; revision received May 26, 1969. The authors acknowledge the contributions of the investigators listed in Table 2. We would like to express special appreciation to L. Lanzerotti and C. Bostrom who with short notice furnished key data and whose over-all cooperation contributed considerably to the study.

* Physicist, Space Sciences Department, Western Division.
† Deputy Chief Scientist, Space Sciences Department, Western Division.

Table 1 Solar cosmic ray events

Date	Flare max.	Imp	Coord	X-ray start	SCNA[a] start	Type IV start	Intensity, cm^{-2}	Dose, rad
28 Sept. 61	2225	3	N13E30	[b]	[b]	2212	7.8×10^6 (>30)	2.7
5 Feb. 65	1810	2+	N07W25	[b]	[b]	1810	1×10^7 (>15)	1.9
24 March 66	0238	3B	N22W42	[b]	0218	[b]	[b]	4.7
7 July 66	0041	3B	N34W47	0025	0026	<0053	1.7×10^7 (>15)	2.8
2 Sept. 66	0558	3B	N22W57	0346	0550	[b]	8×10^7 (>30)	100
28 Jan. 67		(not established)		0737	[b]	[b]	2.3×10^8 (>20)	64
23 May 67	1814	2B–3B	N30E25	1808	1809	1537	1.2×10^8 (>25)	65
28 May 67	0546	3B–4B	N28W33	0528	0531	[b]	1.8×10^7 (>30)	4.1

[a] Solar cosmic noise absorption. [b] Insufficient data.

Table 1, along with associated flare parameters, the total proton intensity (having energy greater than that indicated, in Mev) integrated over the duration of the event, and the total calculated dose behind a 1 g cm^{-2} spherical aluminum shield in free space. The very large events that have been observed (e.g., 12 November 1960, 4800 rad, and 14 July 1959, $\geq$2500 rad) occurred before satellite instrumentation was capable of making detailed time histories of energy spectra and hence are not included. The primary data sources for the solar cosmic ray analyses included in this study are given in Table 2.

Model Development

The technique used is to develop event models that fit solar cosmic ray events that have been observed in the past.

Table 2 Data collection and sources

Event	Satellite	Investigators
28 Sept. 61	Explorer 12	D. A. Bryant, T. L. Cline, U. D. Desai, and F. B. McDonald[4]
5 Feb. 65	1963-38C	C. O. Bostrom, J. W. Kohl, and D. J. Williams,[5] and C. O. Bostrom[a]
	IMP-2	F. B. McDonald[a]
	1964-45A	G. A. Paulikas, S. C. Freden, and J. B. Blake[6]
	Injun IV	S. M. Krimigis and J. A. Van Allen[7]
	IMP-2	J. J. O'Gallagher and J. A. Simpson[8]
24 March 66	OGO-1	S. W. Kahler, J. H. Primbsch, and K. A. Anderson[9]
	Neutron monitors	J. A. Lockwood[a]
7 July 66	1963-38C	C. O. Bostrom[a]
	IMP-3, OGO-3, Explorer 33	R. P. Lin, S. W. Kahler, and E. C. Roelof[10]
	Balloons	D. J. Heristchi et al.[11]
	IMP-3	F. B. McDonald[a]
2 Sept. 66	OGO-3	S. W. Kahler and K. A. Anderson[a] E. C. Roelof[a]
	Rockets	C. O. Bostrom[a]
28 Jan. 67	ATS-1	L. J. Lanzerotti[a]
	IMP-3	K. A. Anderson[a]
	ATS-1	G. A. Paulikas[a]
	Neutron monitors	J. A. Lockwood[a]
23 May 67	Vela	S. Singer[a]
	1963-38C	C. O. Bostrom[a]
	IMP-F	J. L. Lanzerotti[a]
	Explorer 34	C. O. Bostrom,[a] and C. O. Bostrom, D. J. Williams, and J. F. Arens[12]
	OGO-3	S. W. Kahler[a]
28 May 67	1963-38C	C. O. Bostrom[a]
	Explorer 34	C. O. Bostrom,[a] and C. O. Bostrom, D. J. Williams, and J. F. Arens[12]

[a] Private communication.

Presumably, events that occur in the future will also fit one of the models. Therefore, when an event occurs, the data can be utilized in real time to make a dose projection. The process would be iterative and continually updated as new data are received, so the projected total dose would approach the true dose ultimately experienced as the number of data points increases. Two types of models have been considered in some detail. Table 3 lists the candidate events and the models. An X under model indicates that the model was applied to that event; an X under dose shows that the analysis was carried through to the point of making a dose projection. Each of the events was analyzed to convert the data into energy spectra as a function of time. The form and completeness of the data varied from event to event, so the amount of actual analysis required also varied. The general techniques used in the analyses are described by Masley and Goedeke.[1]

Epeak Model

In most solar cosmic ray events the higher-energy protons arrive at the earth earlier than the lower energy protons. This velocity dispersion can be seen in Fig. 2, the time history of the intensities of protons during the 7 July 1966 event. One measurable parameter resulting from this dispersion is the time at which the intensity of particles of a particular energy (or in a particular energy band) reaches its peak. Figure 3 shows these peak times for the same event.

Using the time histories shown in Fig. 2, the dose history for the event was calculated[13] and is shown in Fig. 4, for a 1 g cm^{-2} aluminum spherical shield in free space. The dose rate curve was integrated and is plotted in Fig. 5 as cumulative percent dose vs time. Also shown on the same figure are the times when the intensities of protons of a certain energy reached their peak. The percent dose accumulated can now be plotted vs energy of protons reaching peak intensity, as in Fig. 6. It can be seen from Fig. 6 that when the 120 Mev protons, for instance, have reached peak intensity, 7% of the total dose has been received.

The results for the events of 28 September 1961, 5 February 1965, 24 March 1966, and 28 January 1967 also are shown in Fig. 6. Also plotted (as a dashed line) is the estimated

Table 3 Models

Solar cosmic ray event	Epeak		Isotropic diffusion	
	Model	Dose	Model	Dose
28 Sept. 61	X	X	X	X
5 Feb. 65	X	X	X	X
24 March 66	X	X	X	X
7 July 66	X	X	X	X
2 Sept. 66				
28 Jan. 67	X	X	X	X
23 May 67	[a]		X	
28 May 67			X	X

[a] Model inapplicable: no significant velocity dispersion.

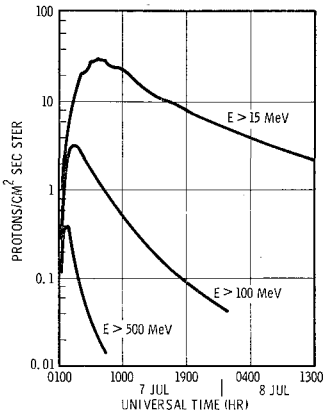

Fig. 2 The free space time-intensity profiles of the 7 July 1966 solar cosmic ray event for various proton energies. Note the logarithmic time scale and the slower rise and decay times with decreasing energy.

best fit straight line,

$$\%D = 29e^{-0.0133(E-20)} \quad (1)$$

The 28 May 1967 event fits this line quite well up to 60 Mev, the highest energy for which we now have suitable data. The 23 May 1967 event could not be included because, within the limits of accuracy of the data, all energies peaked at the same time; i.e., there was no velocity dispersion.

If it is assumed that each event can be described by Eq. (1), then as each measured energy reaches peak intensity

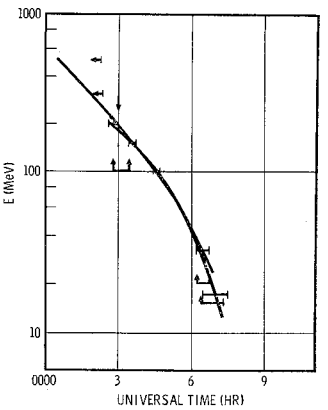

Fig. 3 Energy of the particles reaching maximum intensity vs time (7 July 1966 event).

the percent dose accumulated to that time can be calculated. Thus, if cumulative dose measurements (or calculated doses) are available simultaneously, the expected total dose for the event can be determined. The results of these calculations for the same five events included in Fig. 6 are shown in Figs. 7–11. The actual cumulative dose is plotted vs time, and the projected total doses (marked Epeak) are shown at the times when the protons having energies of 120, 80, 50, 30, and 20 Mev peak. The results for the 24 March 1966 event are

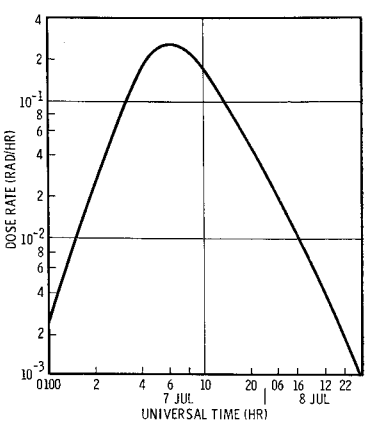

Fig. 4 The free space dose rate, behind 1 g cm^{-2} Al, during the 7 July 1966 event. Note the logarithmic time scale.

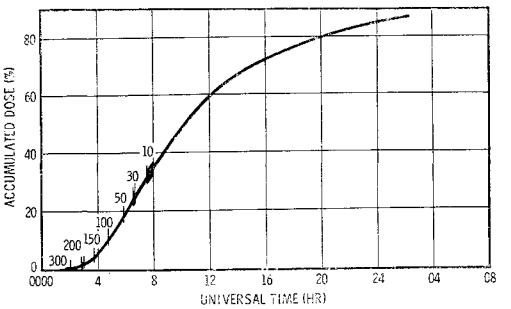

Fig. 5 The percentage of accumulated dose (1 g cm^{-2} Al) vs time during the 7 July 1966 event. Also plotted are the proton energies reaching maximum intensity (see Fig. 3).

rather poor, the 28 January 1967 event results are high by a factor of two at first, and the others are quite good.

These projections can be improved for all but the first point by using

$$\%D = 29e^{-B(E-20)} \quad (2)$$

where

$$B = [1/(E_1 - E_2)] \ln(X_2/X_1) \quad (3)$$

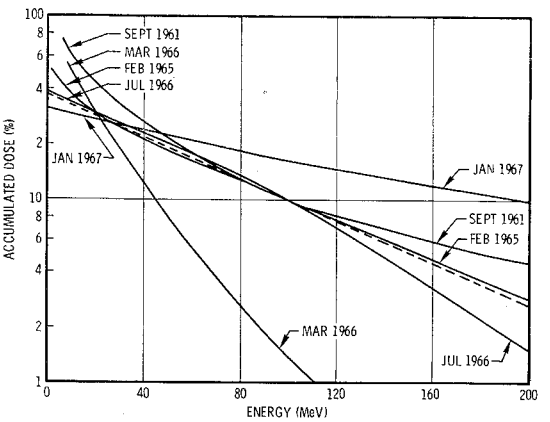

Fig. 6 The percentage of accumulated dose behind 1 g cm^{-2} Al vs the energy of particles reaching maximum intensity for various events. These curves were constructed by the use of Figs. 3 and 5 for the 7 July 1966 event and corresponding curves for the other events. Also shown as a dashed line is the empirical relationship given as Eq. (1).

E_1 = 120 Mev, E_2 = 80 Mev, X_1 = true accumulated dose when E_1 is peaking, and X_2 = true accumulated dose when E_2 is peaking.

This amounts to allowing the dashed curve in Fig. 6 to pivot around the E = 20 Mev point, and calculating the

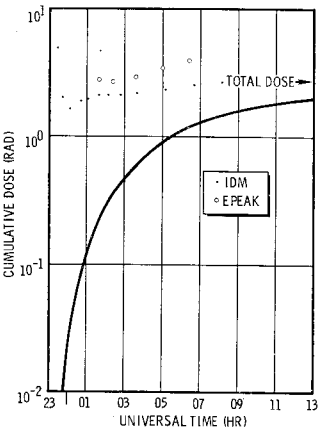

Fig. 7 The cumulative dose behind 1 g cm^{-2} Al vs time (solid line). Also shown are the projections of the total dose by the two methods outlined in this paper. IDM denotes the isotropic diffusion model.

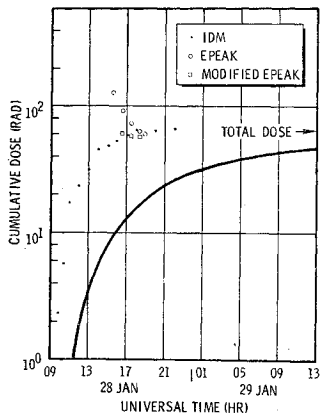

Fig. 8 Cumulative dose (28 Jan. 1967 event). The same as Fig. 7 except that the modified Epeak method is also shown (see text for description of the methods).

slope from the first two measurements. The results of using Eqs. (2) and (3) are shown in Figs. 8 and 9 (marked modified Epeak). The improvement in these two cases is obvious; no significant changes were made in the other three cases.

Difficulties with this model are associated with the actual measurement of the peak times. Distinct energies are usually not observed with a spectrometer, only somewhat

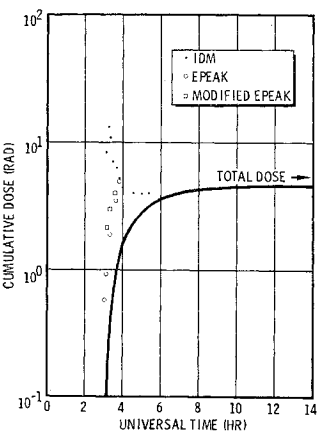

Fig. 9 Cumulative dose (24 March 1966 event). The same as Fig. 7.

broad energy bands; furthermore, the fine structure in the time history of particle events combined with wide peaks (typically of the order of an hour or more) will cause a time lag in determining when the peak actually occurs. These two effects contribute to uncertainties in the dose expected.

Isotropic Diffusion Model

The second model considered is based on isotropic diffusion theory.[14–16] Figure 12 can be used to describe the method,

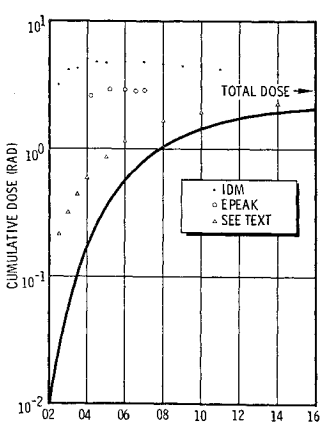

Fig. 10 Cumulative dose (7 July 1966 event). The same as Fig. 7.

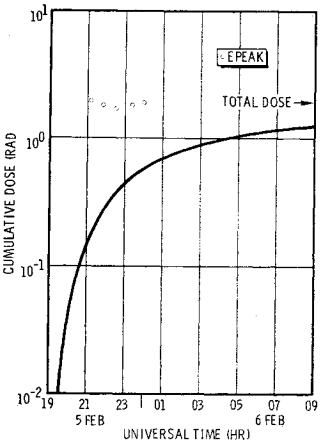

Fig. 11 Cumulative dose (5 Feb. 1965 event). The same as Fig. 7, except using only the Epeak method.

where F is the proton intensity (usually cm^{-2} sec^{-1}), T is the time in hours after T_0 (the time of particle injection at the sun), and β is a parameter (usually set equal to 1.0) related simply to the diffusion coefficient. The theory predicts that (F,T) data points plotted as shown in Fig. 12 should fall on a straight line. Therefore, as soon as two data points are measured they are plotted as shown (assuming T_0 to be either one hour before T_1 or the known injection

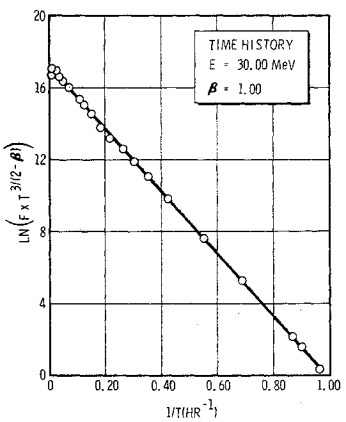

Fig. 12 Isotropic diffusion model (28 Sept. 1961 event). The time-intensity profile of the 30 Mev protons during the 28 Sept. 1961 event plotted in the coordinate system in which the points should fall on a straight line. β is related to the diffusion coefficient.

time) and a straight line passed through the points. The slope of the line and the Y intercept (at $1/T = 0$) are then used to calculate the projected time history of the event (as shown in Fig. 13), the total time-integrated intensity expected, and the time of occurrence of the peak intensity. This is repeated for all energies for which data are available, and the resulting time-integrated energy spectrum used to calculate the total expected dose. As each subsequent data point is input, the entire process is repeated, with one addition: the straight line (as shown on Fig. 12) is fitted to the data using a least-squares routine, then T_0 is incremented if the

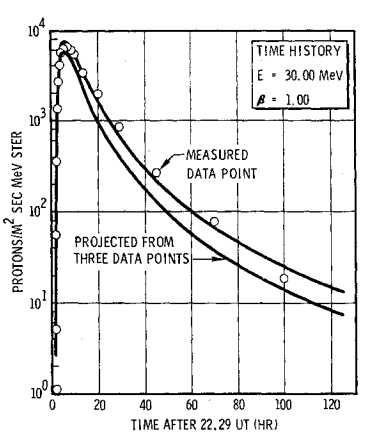

Fig. 13 The time-intensity profile of the 30 Mev protons during the 28 Sept. 1961 event displayed along with the projection of the event using the first three data points to draw a curve like that shown in Fig. 12.

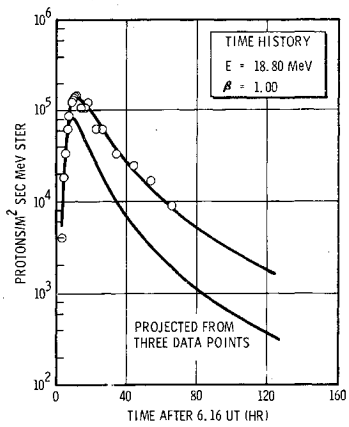

Fig. 14 Time-intensity profile (28 Jan. 1967 event). Same as Fig. 13, except for 18.8 Mev protons.

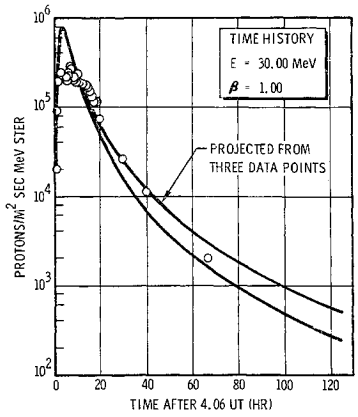

Fig. 16 Time-intensity profile (28 May 1967 event). Same as Fig. 13.

injection time is not known and a straight line again fitted to the data. This is continued until the sum of the residuals is minimized.

In Fig. 13, the time history of the 28 September 1961 event 30 Mev protons as projected from three data points is the lower curve; the best fit to all the data points is the upper curve; and the actual data points are shown by open circles. The projections for the events of 28 January 1967, 23 May 1967, and 28 May 1967 are shown in Figs. 14–16 (in each case, for only one energy). Figure 7 presents the final results of the projections for the 28 September 1961 event (marked IDM). The first dot is based on two data points, the second on three, etc. For this event, the results are very good; accurate estimates of the expected total dose would have been available at least two hours before the intensity of 120 Mev protons had reached its peak. The results of the analysis for 28 January 1967 (Fig. 8) are not as good, but three hours before the 120 Mev peak the total dose predicted is less than a factor of four low. The 24 March 1966 event (Fig. 9) was so brief that no time advantage is afforded by the isotropic diffusion model over the Epeak model.

The 7 July 1966 event showed an interesting effect. When the injection at the sun was assumed to occur during the obvious flare, the results of the analysis are shown as triangles in Fig. 10. If, however, the injection time is calculated by the program, the results are shown as points. This calculated injection time was 2239 universal time on 6 July, some two hours before the flare. This is the only case (other than 28 January 1967, when no large flare was observed) when the program consistently calculated an injection time significantly different from the time of optical maximum or type IV start.

For the 28 May 1967 event, Fig. 17, the predicted total dose is never as much as a factor of five different from the true dose. For the 23 May 1968 event projections of the total time-integrated intensity of protons having $E > 8.4$ Mev were calculated and the estimates differed from the true value by up to three orders of magnitude. This is what one might expect, considering the poor fit of the model time history to the actual time history of the event. This event differs from the other types considered due to its very slow rise time, fast decay, and small velocity dispersion. The isotropic diffusion model could not be expected to fit this type of event.

As can be seen from the foregoing results, the isotropic diffusion model represents another good model candidate. Several refinements can be made to improve it, among which are the following:

1) Only two values of β have been used so far, one of which ($\beta = 0$) gave poor results. In several cases a better fit to the data could have been made by changing β slightly.

2) The values of T_0 computed by the program for different proton energies in the same event are not intercompared. If the injection time at the sun is known (for instance from solar radio or optical observations) this can be input and the iteration of T_0 suppressed, but if is not accurately known the injection times for the different energies should at least not be completely independent.

3) No provision is made for the dependence of event time history on solar longitude of the flare; this must be included because the propagation of particles between the sun and the earth cannot be expected to be adequately described by an isotropic diffusion model for all injection longitudes. This is seen to be the case for the May 23, 1967 event for instance.

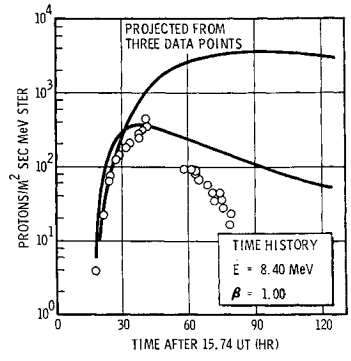

Fig. 15 Time-intensity profile (23 May 1967 event). Same as Fig. 13, except for 8.4 Mev protons. The peculiar time-intensity profile of this event prevents the model from accurately projecting the event.

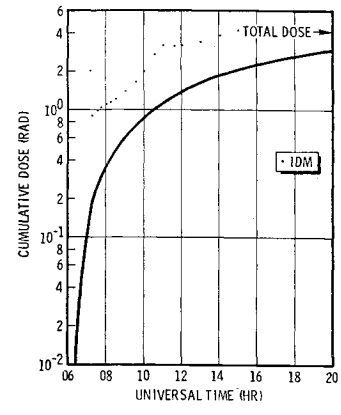

Fig. 17 Cumulative dose (27 May 1967 event). The same as Fig. 7, except using only the IDM model.

References

[1] Masley, A. J. and Goedeke, A. D., "Complete Dose Analysis of the November 12, 1960, Solar Cosmic Ray Event," *Life Sciences and Space Research*, edited by R. B. Livingston, A. A. Imshenetsky, and G. G. Derbyshire, North-Holland, Amsterdam, 1963, pp. 95–109.

[2] Webber, W. R., "An Evaluation of the Radiation Hazard Due to Solar-Particle Events," D2-90469, Dec. 1963, The Boeing Co., Seattle, Wash.

[3] Kane, S. R. and Winckler, J. R., "The Critical Analysis of Balloon Flights at Minneapolis During the November 1960 Cosmic Ray Flare Events," TR CR-124, Jan. 1969, School of Physics and Astronomy, Univ. of Minnesota, Minneapolis, Minn.

[4] Bryant, D. A. et al., "Explorer 12 Observations of Solar Cosmic Rays and Energetic Storm Particles after the Solar Flare of September 28, 1961," *Journal of Geophysical Research*, Vol. 67, No. 13, Dec. 1962, pp. 4983–5000.

[5] Bostrom, C. O., Kohl, J. W., and Williams, D. J., "The February 5, 1965 Solar Proton Event 1. Time History and Spectrums Observed at 1,100 km," *Journal of Geophysical Research*, Vol. 72, No. 17, Sept. 1967, pp. 4487–4495.

[6] Paulikas, G. A., Freden, S. C., and Blake, J. B., "Solar Proton Event of February 5, 1965," *Journal of Geophysical Research*, Vol. 71, No. 7, April 1966, pp. 1795–1798.

[7] Krimigis, S. M. and Van Allen, J. A., "Observations of the Solar Particle Event of 5 to 12 February 1965 with Mariner IV and Injun IV," *Journal of Geophysical Research*, Vol. 72, No. 17, Sept. 1967, pp. 4471–4486.

[8] O'Gallagher, J. J. and Simpson, J. A., "Anisotropic Propagation of Solar Protons Deduced from Simultaneous Observations by Earth Satellites and the Mariner-IV Space Probe," *Physical Review Letters*, Vol. 16, No. 26, June 1966, pp. 1212–1217.

[9] Kahler, S. W., Primbsch, J. H., and Anderson, K. A., "Energetic Protons from the Solar Flare of March 24, 1966," *Solar Physics*, Vol. 2, No. 2, 1967, pp. 179–191.

[10] Lin, R. P., Kahler, S. W., and Roelof, E. C., "Solar Flare Injection and Propagation of Low-Energy Protons and Electrons in the Event of 7–9 July 1966," *Solar Physics*, Vol. 4, No. 3, July 1968, pp. 338–360.

[11] Heristchi, D. J. et al., "Balloon Measurements of Solar Protons in Northern Scandinavia on 7 July 1966," *Annals of the IQSY*, Paper 38, M.I.T. Press, 1969.

[12] Bostrom, C. O., Williams, D. J., and Arens, J. F., "Solar-Geophysical Data," IEF-RB-282, Feb. 1968, U.S. Dept. of Commerce Environmental Science Service Administration, Boulder, Colo., p. 156.

[13] Lilley, J. R. and Yucker, W. R., "CHARGE, a Space Radiation Shielding Code," Rept. DAC-62231, May 1969, McDonnell Douglas Astronautics Co.

[14] Krimigis, S. M., "Interplanetary Diffusion Model for the Time Behavior of the Intensity in a Solar Cosmic Ray Event," *Journal of Geophysical Research*, Vol. 70, No. 13, July 1965, pp. 2943–2960.

[15] Parker, E. N., *Interplanetary Dynamical Processes*, Interscience, New York, 1963.

[16] Hofmann, D. J. and Winckler, J. H., "Simultaneous Balloon Observations at Fort Churchill and Minneapolis during the Solar Cosmic Ray Events of July 1961," *Journal of Geophysical Research*, Vol. 68, No. 8, April 1963, pp. 2067–2098.

NOVEMBER 1969 AIAA JOURNAL VOL. 7, NO. 11

Nutation Damper Instability on Spin-Stabilized Spacecraft

GERALD J. CLOUTIER*
Itek Corporation, Lexington, Mass.

The dynamic equations describing the motion of a single-degree-of-freedom nutation damper mounted on a dual-spin spacecraft are examined. The motion of the damper mass is found to be parametrically excited by the transverse angular rates, so that instabilities of this motion are possible. In this situation, instability could imply that the damper mass moves to an extreme position and remains there; hence, it would not perform its intended function of dissipating energy in order to damp out nutation. It is found that this unstable behavior is quite possible for a damper mounted on a single-spin spacecraft or on the spinning portion of a dual-spin spacecraft where the other member is essentially despun. On the other hand, unstable behavior of a damper mounted on the despun member of a dual-spin configuration is found to be extremely unlikely.

Nomenclature

A, C = moments of inertia, slug ft^2 (ft-lb-sec^2)
D = angular momentum ratio
H = angular momentum, ft-lb-sec
M = moment, ft-lb
P = amplitude of angular velocities, rad/sec
a = acceleration, ft/sec^2
b = length, ft
c = damping constant, lb-sec/ft
d,e = parameters
f_n = natural frequency, rad/sec
k = spring constant, lb/ft
m = mass, slugs (lb-sec^2/ft)
v = velocity, fps
δ,ϵ = parameters
ζ = damping ratio
θ = wobble angle, rad
μ = characteristic exponent
τ = nondimensional time
Ω = precessional frequency, rad/sec
ω = angular velocity, rad/sec

Received October 27, 1968; revision received June 27, 1969. Most of the work reported here was performed while the author was employed at Sylvania Electronic Systems, Waltham, Mass.

* Senior Aeronautical Engineer, Optical Systems Division. Member AIAA.

Introduction

MANY passive nutation dampers (passive implying that the damper is driven by the coning motion of the spacecraft) have been proposed for eliminating undesirable nutational motions of spin-stabilized spacecraft.[1–3] The analyses for most of these designs involve many approximations and linearizations, since they are intended to provide design guidelines for the dampers. However, some analysts have examined the complete set of equations for certain dampers and have uncovered nonlinear and even unstable forms of motion.[4,5] An important aspect of any damper application, then, is the study of any possible nonlinear behavior or instability in its motion. In this paper, a very simple, one-degree-of-freedom, mass-spring-dashpot damper is analyzed. This type of damper has been studied previously (by a linearized analysis) for a single-spin system,[6] but in the present case, the analysis is expanded to include dual-spin systems, i.e., spacecraft consisting of two major bodies which rotate relative to one another about a common